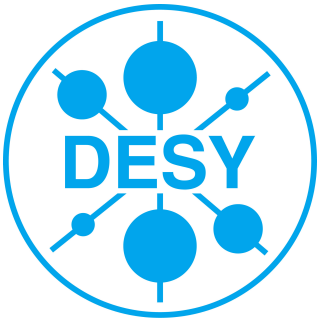

Higgs-strahlung in the Two-Higgs-Doublet-Model (THDM)

Margarita Gavrilova, Moscow Institute of Physics and Technology (State University)

September 6, 2017

Abstract

This report, in the context of the DESY Summer Student Program 2017, presents a phenomenological study of the $pp \to A \to Zh$ process (so called Higgs-strahlung) in the THDM. In this report, we are giving a brief theoretical overview of the THDM. The parameter dependence of the THDM relevant to the process is studied numerically (with help of `SusHi` and `2HDMC` software). Also, we have performed an analytical and numerical calculation of the cross section at leading order (LO) and a numerical calculation at next-to-leading order (NLO) and next-to-next-to-leading order (NNLO).

Group : DESY theory group
Supervisors : Stefan Liebler, Emanuele Bagnaschi, Georg Weiglein

Contents

1 Introduction

Since the discovery of a Higgs boson in 2012 one of the most important task for particle physics is to reveal its nature. This stands for studying Higgs production and decay modes in order to understand if the particle we observe is the Standard Model (SM) Higgs boson or not.

However, what we know for sure today – the SM is an incomplete model. This conclusion follows first of all from our observations. For example, there is no dark matter candidate in the SM, while according to the nowadays data more than 20% of the Universe is dark matter. Other problems are the baryon asymmetry which can not be fully explained by means of the SM and, for instance, gravity which is basically not present in the current model of particle physics. Also, there are some pure theoretical issues such as the hierarchy problem or strong CP problem.

That is why besides characterizing the known Higgs boson there is another interesting research avenue – to study how other possible Higgs-states in different SM extensions could appear at the LHC. In this project we focus on one of the simplest possible extensions of the SM – the Two-Higgs-Doublet-Model (THDM) and particularly on the Higgsstrahlung process (the production of a Higgs together with a gauge boson). Despite it is not the most dominant Higgs production mechanism it is of large relevance due to several aspects. Firstly, because of the presence of the gauge boson, which can be tagged in the final state. Secondly, the important decay of Higgs boson to bottom quarks is experimentally accessible in this channel. Moreover the gluon-fusion component $gg \to Zh$ is very sensitive to new physics. Lastly, in extended Higgs sectors, both the gluon-fusion component $gg \to Zh$ as well as the $b\bar{b} \to Zh$ contribution can be resonantly enhanced by internal (pseudo)scalars. This latter process was only rudimentary studied in previous work [7] and therefore deserves some more attention. Thus, it is the aim of this project to study the process $b\bar{b} \to A \to Zh$ beyond its prediction at leading order (LO) in perturbation theory, as it is available in literature.

In this report, we are giving a brief overview of the THDM (see Section 2), performing a numerical study of A–decays in the THDM (Section 3) and present an analytical calculation of $pp \to A \to Zh$ cross section at LO and a numerical calculation up to NNLO (Sections 4-5).

2 Two Higgs Doublet Model (THDM)

There are many motivations for THDMs. The best known motivation is supersymmetry which in its minimal version requires two Higgs doublets. Another advantage of the THDM is the fact that this model potentially can generate the necessary amount of CP violation which is observed in nature and also might have some dark matter candidate [1].

In principle the Higgs sector in the THDM works exactly like in SM but instead of one Higgs doublet now we have two of them. This of course leads to some complications. First of all we need to consider a different potential. After the requirement of a few simplifications such as no CP-violation in the Higgs sector and no flavour-changing neutral currents the potential involving two Higgs doublets Φ_1 and Φ_2 takes the

form:

$$V(\Phi_1,\Phi_2) = m_{11}^2\Phi_1^\dagger\Phi_1 + m_{22}^2\Phi_2^\dagger\Phi_2 - m_{12}^2\left(\Phi_1^\dagger\Phi_2 + \text{h.c}\right) + \frac{\lambda_1}{2}\left(\Phi_1^\dagger\Phi_1\right)^2 + \frac{\lambda_2}{2}\left(\Phi_2^\dagger\Phi_2\right)^2 \\ +\lambda_3\Phi_1^\dagger\Phi_1\Phi_2^\dagger\Phi_2 + \lambda_4\Phi_1^\dagger\Phi_2\Phi_2^\dagger\Phi_1 + \frac{\lambda_5}{2}\left[\left(\Phi_1^\dagger\Phi_2\right)^2 + \text{h.c}\right]. \tag{1}$$

After electroweak symmetry breaking the neutral components of the two Higgs doublets develop vacuum expectation values as follows:

$$\langle\Phi_1\rangle_0 = \frac{1}{\sqrt{2}}\begin{pmatrix}0\\v_1\end{pmatrix}, \qquad \langle\Phi_2\rangle_0 = \frac{1}{\sqrt{2}}\begin{pmatrix}0\\v_2\end{pmatrix} \tag{2}$$

Expanding the two Higgs doublets around these vacuum expectation values yields four real fields for each of the Higgs doublet:

$$\Phi_a = \begin{pmatrix}\phi_a^+\\ \left(v_a + \rho_a + i\eta_a\right)/\sqrt{2}\end{pmatrix}, \qquad a = 1,2 \tag{3}$$

In the neutral sector this includes the CP-even component ρ_a and the CP-odd component η_a. Three of eight fields give mass to Z^0 and $W^\pm$ gauge bosons, while the remaining five are physical Higgs states. Finally in this model there are two charged scalars, two neutral scalars and one pseudoscalar.

Substituting the doublets (3) in the potential (1) we get mass terms Eqs. (4) - (6). For charged scalars:

$$\mathcal{L}_{\phi^\pm}^{\text{mass}} = \left[m_{12}^2 - (\lambda_4+\lambda_5)v_1v_2\right]\left(\phi_1^-,\phi_2^-\right)\begin{pmatrix}\frac{v_2}{v_1} & -1\\ -1 & \frac{v_1}{v_2}\end{pmatrix}\begin{pmatrix}\phi_1^+\\ \phi_2^+\end{pmatrix}. \tag{4}$$

The mass terms for the pseudoscalars:

$$\mathcal{L}_\eta^{\text{mass}} = \frac{M_A^2}{v_1^2+v_2^2}\left(\eta_1,\eta_2\right)\begin{pmatrix}v_2^2 & -v_1v_2\\ -v_1v_2 & v_1^2\end{pmatrix}\begin{pmatrix}\eta_1\\ \eta_2\end{pmatrix}, \quad M_A^2 = \left[m_{12}^2/(v_1v_2) - 2\lambda_5\right]\left(v_1^2+v_2^2\right). \tag{5}$$

Finally, the mass terms for the neutral scalars:

$$\mathcal{L}_\rho^{\text{mass}} = -\left(\rho_1,\rho_2\right)\begin{pmatrix}m_{12}^2\frac{v_2}{v_1} + \lambda_1v_1^2 & -m_{12}^2 + \lambda_{345}v_1v_2\\ -m_{12}^2 + \lambda_{345}v_1v_2 & m_{12}^2\frac{v_1}{v_2} + \lambda_1v_2^2\end{pmatrix}\begin{pmatrix}\rho_1\\ \rho_2\end{pmatrix}, \quad \lambda_{345} = \lambda_3+\lambda_4+\lambda_5. \tag{6}$$

In order to move to the physical basis, the scalar mass-squared matrix should be diagonalized, thus we introduce a new model parameter - rotation angle α. The mass eigenstates of the CP-even sector are called h and H and their masses M_h and M_H respectively. Another important parameter of the THDM is

$$\tan\beta = \frac{v_2}{v_1}. \tag{7}$$

The angle β is the rotation angle which diagonalizes the mass-squared matrices of charged scalars and of pseudoscalars.

Rather than employing the λ_i basis we use the physical basis:

$$M_h, M_H, M_A, M_{H^\pm}, \tan\beta, \sin\left(\alpha-\beta\right), m_{12}^2. \tag{8}$$

Its input is based on the masses of all five Higgs bosons, the ratio (7), the CP-even mixing angle α in the form $\sin(\alpha-\beta)$ and m_{12}^2.

In this project the subject of our study is the THDM process with joint production of a light Higgs h and Z boson and particularly the diagram in Fig. 3. In the physical basis the relevant couplings for the process $b\bar{b} \to A \to Zh$ depend on the mixing angles α and β. We normalize all couplings to the SM strength and just write relative couplings g. We refer to [7] for the notation.

$$g_{A\bar{d}d} = \tan\beta, \;\; g_{A\bar{u}u} = \frac{1}{\tan\beta} \\ g_{AZh} \sim \cos\left(\alpha-\beta\right) \\ g_{AW^\pm H^\mp} = 1 \tag{9}$$

The last coupling $g_{AW^\pm H^\mp}$ does not occur in the process directly, but will indirectly enter our analysis through the decay width of the pseudoscalar A.

The essential requirement for any beyond the SM theory is its consistency with the current experimental situation. For example in the THDM $e^-e^+ \to Z \to Zh$ cross section is given by:

$$\sigma_{\text{THDM}} = \sin^2(\alpha - \beta)\, \sigma_{\text{SM}}. \tag{10}$$

Consequently for the light Higgs h to have SM properties the coupling $\sin(\alpha - \beta)$ has to be close to 1. Accordingly $\cos(\alpha - \beta)$ remains close to 0. [9]

3 Study of A decays in the THDM

In this section, we perform a numerical study of A decays to see clearly model's dependence on the parameter choice. To conduct this numerical study we used `SusHi` and `2HDMC` codes. For more details on the numerical calculation see Section 5.

For our research we have chosen three pseudoscalar masses 250, 400 and 1000 GeV. The values of the other parameters can be found in Table 1.

M_A, GeV	M_b, GeV	M_h, GeV	m_{12}, GeV	$M_{H^\pm}$, GeV	M_H, GeV	$\tan\beta$	$\sin(\alpha-\beta)$
250	2.883118	125	100	271.512	316.465	0.5 .. 60	-1 .. 1
400	2.798037						
1000	2.651288						

Table 1: THDM parameter values for numerical study

Here M_b is the bottom mass for the Yukawa coupling in the $\overline{\text{MS}}$ renormalization scheme chosen at the pseudoscalar scale M_A. One can feel free choosing a heavy Higgs mass M_H and charged Higgs mass $M_H^\pm$, since our analysis is essentially insensitive to those paremeters as long as these decays do not affect the A decay width.

Fig. 1 represent our results. The first observation one can do is that the decay width increases with M_A. This is expected since the higher the particle mass the more decay channels open. Another noticeable thing about our results is different decay width patterns for $M_A = 250$ GeV and higher masses. The pattern for decay width at 250 GeV can be explained by two factors. Firstly, since $g_{Ab\bar{b}} \sim \tan\beta$ we see the increase of the total decay width and $\text{BR}(A \to b\bar{b})$ with $\tan\beta$. Secondly $g_{AZh} \sim \cos(\alpha-\beta)$, which explains the curvature of the A decay width. At $\cos(\alpha - \beta) = 0$ the branching ratio of $A \to Zh$ vanishes.

The situation is different for higher masses $M_A = 400$ GeV and $M_A = 1000$ GeV. In these cases also the decay $A \to t\bar{t}$ is kinematically open and thus also influences the behavior of all other branching ratios. As we mentioned before $g_{At\bar{t}} \sim (\tan\beta)^{-1}$. That is why we observe high values of the total decay width at small $\tan\beta$. The simultaneous participation of three factors we discussed is finally giving us this onion-like structure.

For $M_A = 1000$ GeV our parameter choice with a low (compared to M_A) charged Higgs mass allows for the decay $A \to W^\pm H^\mp$ to be kinematically open. Its branching ratio is shown in Fig. 2. But since the coupling for this decay has no β or α dependence this process does not influence the pattern we see. It just contributes to the total decay width (as one can see from Fig. 1 at 1000 GeV the pseudoscalar has a very large total decay width).

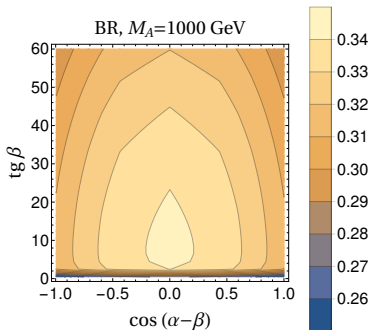

Figure 2: Branching ratio of $A \to W^\pm H^\mp$ decay at $M_A = 1000$ GeV

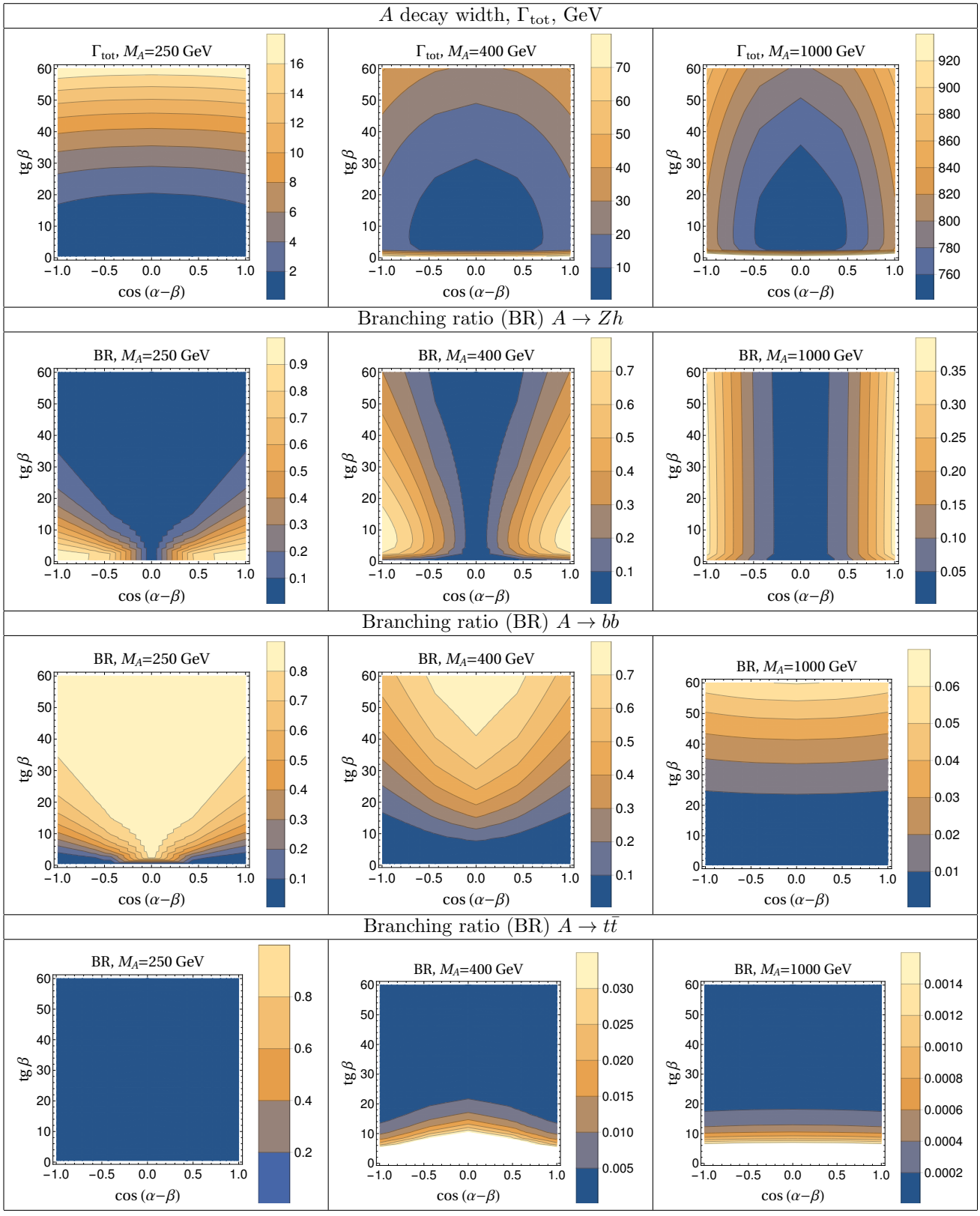

Figure 1: Numerical study of A decays in THDM

In sections 4 and 5 we perform a cross section calculation for the studied process. To do so for each mass we have chosen a point in the $(\cos(\alpha-\beta), \tan\beta)$ plane. Our choice is represented in Table 2.

M_A, GeV	250	400	1000
$\tan\beta$	2	6	5
$\sin(\alpha-\beta)$	0.6	0.8	0.9

Table 2: Points in parameter space used in the cross section calculation

4 Analytical calculation of $b\bar{b} \to A \to Zh$

In this section we are going to provide an analytical calculation of the cross section for $b\bar{b} \to A \to Zh$ process at tree level. The Feynman graph corresponding to the process is shown in Fig. 3.

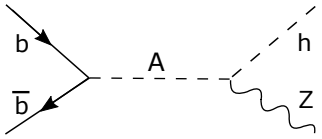

Figure 3: Feynman diagram for the $b\bar{b} \to A \to Zh$ process

We used FeynArts to choose our Feynman graph topology and generate the amplitude (11) of the process:

$$M = \delta_{rs} \sum_{r=1}^{3} \sum_{s=1}^{3} \bar{v}_b^r(p_2) \frac{-eM_b Y_3}{4M_W \cos\theta_W \sin^2\theta_W} \gamma_5 u_b^s(p_1) \frac{e\cos(\alpha-\beta)}{(k_1+k_2)^2 - M_A^2 - iM_A\Gamma_A} (-k_1-2k_2)^\mu e_Z^\mu(k_1). \quad (11)$$

In (11): p_1, p_2 — quarks momenta; k_1 — Z–boson momentum; k_2 — Higgs momentum; $s = (p_1+p_2)^2 = (k_1+k_2)^2$ — quark center of mass energy squared; r, s — color indexes; v, u — quark spinors; e^μ — polarization vector of Z–boson; e — electron charge; $Y_3 = \tan\beta$ — normalized bottom Yukawa coupling; M_A — pseudoscalar mass; Γ_A — pseudoscalar decay width; M_W — W–boson mass; θ_W — electroweak mixing angle; M_b — bottom mass in $\overline{MS}$ scheme at the scale of M_A. Throughout this report we assumed initial state quarks to be massless. The bottom–quark mass is only taken into account in the bottom–quark Yukawa coupling.

In order to get the matrix element which we initially need to derive the cross section we used FormCalc to square the amplitude (11) and perform the sum over final state polarization, color and helicity averaging. As a result we got the following expression for the matrix element squared:

$$|M|^2 = \frac{3\pi^2 \alpha_{\text{fine str}}^2 \cos(\beta-\alpha)^2 M_b^2 \frac{Y_3^2}{M_Z^2} s \left(-2M_h^2\left(s+M_Z^2\right) + M_h^4 + \left(s-M_Z^2\right)^2\right)}{9 \times 2\cos^2\theta_W M_W^2 \sin^4\theta_W \left(\left(s-M_A^2\right)^2 + M_A^2\Gamma_A^2\right)}. \quad (12)$$

The expression for the cross section is given by (13) (see, for example, [8]). We took into account the fact that in our case there is no angular dependence and expressed the outgoing particle momenta in terms of Mandelstam variable s and masses.

$$\sigma(b\bar{b} \to A \to Zh) = \frac{|M|^2}{8\pi s\sqrt{s}} \times \sqrt{\frac{(M_Z^2 - M_h^2 + s)^2}{4s} - M_Z^2} \quad (13)$$

However expression (13) is still not the answer we are interested in. The point is that real physical event is not the quark collision but a collisions of hadrons, for example, proton-proton collisions. Quarks in the proton are characterized by Parton Distribution Functions (PDFs). Therefore we have to convolve our partonic cross section $b\bar{b} \to A \to Zh$ with the PDFs in order to obtain the hadronic cross section $pp \to A \to Zh$. This involves two integrations over the momentum fractions of the b-quarks in the proton, named x_1 and x_2:

$$\sigma\left(pp \to A \to Zh\right) = 2 \int_0^1 dx_1 dx_2\ \theta\left(\hat{s}x_1x_2 - \left(M_h + M_Z\right)^2\right)\ f_b\left(x_1, Q\right) f_{\bar{b}}\left(x_2, Q\right)\ \sigma\left(b\bar{b} \to Zh\right)\left(\hat{s}x_1x_2\right) \quad (14)$$

Here f_b and $f_{\bar{b}}$ are parton distribution functions for quark and antiquark respectively. Also we used the fact that $s = \hat{s}x_1x_2$ (neglecting the bottom mass), where s - quark center of mass energy and $\hat{s}$ - hadronic center of mass energy. Theta function in Eq. (14) represent the condition for the process to be kinematically open.

For our future studies we are also interested in obtaining the analytical expression for $\frac{d\sigma}{d\sqrt{s}}$. To do this we are performing the following variable transformation:

$$\begin{gathered} x_1 = \sqrt{\frac{s}{\hat{s}}}e^{y},\ x_2 = \sqrt{\frac{s}{\hat{s}}}e^{-y} \\ J = \begin{vmatrix} \frac{1}{\sqrt{\frac{s}{\hat{s}}}}e^{y} & -\frac{1}{\sqrt{\frac{s}{\hat{s}}}}e^{-y} \\ \frac{1}{2\sqrt{\hat{s}s}}e^{y} & \frac{1}{2\sqrt{\hat{s}s}}e^{-y} \end{vmatrix} = \frac{1}{\hat{s}} \quad \Rightarrow \quad dx_1 dx_2 = \frac{1}{\hat{s}} ds dy = \frac{2\sqrt{s}}{\hat{s}} d\sqrt{s} dy. \end{gathered} \tag{15}$$

Which leads us to the expression (16) for the cross section derivative:

$$\frac{d\sigma(pp \to Zh)(s)}{d\sqrt{s}} = \frac{4\sqrt{s}}{\hat{s}} \sigma(b\bar{b} \to Zh)(s) \int_{-\infty}^{\infty} dy f_b\left(\sqrt{\frac{s}{\hat{s}}}e^{y}\right) f_{\bar{b}}\left(\sqrt{\frac{s}{\hat{s}}}e^{-y}\right). \tag{16}$$

5 Higher-order improved result based on a generalized narrow-width approximation

In this section we want to compare our analytical result of Sect. 4 with a generalized narrow-width approximation using numerical codes for the production $pp \to A$ and the decay $A \to Zh$. The employed software packages are:

1. `SusHi` - program which allows to calculate the $b\bar{b} \to A$ cross section up to NNLO. All model parameters such as Higgs mass M_h, pseudoscalar mass M_A, $\tan\beta$ and $\sin(\alpha - \beta)$ are input for the program [5] [6].

2. `2HDMC` - allows to calculate decay width and branching ratios for different A decay channels. [4]

In Table 3 we show the result of our analytical calculation for the three benchmark points. For this purpose we used the standard Mathematica routine NIntegrate to perform the integral in Eq. (14) and the package `ManeParse` [3] to extract the `PDF4LHC15_nlo_mc` PDF set from `LHAPDF` [2]. We also called `SusHi` and `2HDMC` through the call of a `SusHi` input file, that at the same time generates the cross section through bottom-quark annihilation $pp \to A$ as well as a `2HDMC` output file, which contains the relevant branching ratio $A \to Zh$ as well as the employed total decay width.

Here we would like to highlight that in order to obtain the analytical result, which can be compared correctly with the numerical result based on the narrow width approximation, one should be very careful with the input parameters. In particular the choice of the renormalization scheme for the bottom-quark mass entering the Yukawa coupling is very important. In order to minimize the size of higher-order corrections we follow the strategy employed in bottom-quark annihilation and choose the $\overline{\text{MS}}$ bottom-quark mass at the scale of M_A. For electroweak parameters we substituted their values at M_Z. Influence of the scale choice is shown on Fig. 4. To create this graph we run `SusHi` and `2HDMC` for different renormalization scales (from $\frac{1}{2}M_A$ to $2M_A$) and factorization scales (from $\frac{1}{8}M_A$ to $\frac{1}{2}M_A$). As one can see at higher order in perturbation theory the scale dependence is less pronounced, which indicates the convergence of the perturbative series.

To get the numerical cross section based on the narrow width approximation we just multiplied `SusHi` and `2HDMC` outputs as shown below:

$$\sigma_{\text{SusHi + 2HDMC}} = \sigma(b\bar{b} \to A)_{\text{SusHi}}(M_A) \times \text{BR}(A \to Zh)_{\text{2HDMC}}(M_A). \tag{17}$$

M_A, GeV	Γ_A, GeV	$\sigma_{\text{analytical}}$, pb	$\sigma_{\text{SusHi + 2HDMC}}$	Ratio
250	0.425013	0.167540	0.167587	0.999718
400	8.188970	0.135506	0.138187	0.980601
1000	756.506014	0.000114	0.000175	0.649590

Table 3: Comparison of analytical and numerical solutions in LO

Table 3 shows the comparison of our analytical calculation with the application of the narrow width approximation using the cross section and branching ratio from `SusHi` and `2HDMC` respectively. The ratios for $M_A = 250$ GeV and $M_A = 400$ GeV are close to unity. The slight deviation most probably caused by the choice of electroweak parameters in the expression for the matrix element squared (12). The ratio

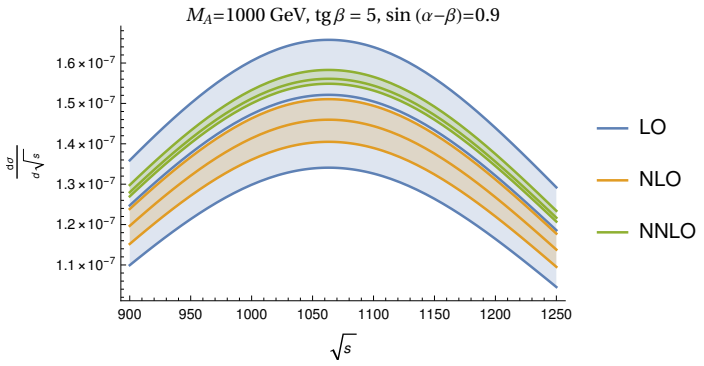

Figure 4: Scale dependence for LO, NLO and NNLO calculations

for $M_A = 1000$ GeV noticeably differs from unity because of the large decay width, when narrow width approximation can not be used anymore.

Using the results of both `SusHi` and `2HDMC`, and applying the approximation formula (18) or its improved variant (19) one can also calculate $\frac{d\sigma}{d\sqrt{s}}$:

$$\frac{d\sigma(b\bar{b} \to Zh)}{d\sqrt{s}} = \sigma(b\bar{b} \to A)(m_A) \frac{2\sqrt{s}}{(s - m_A^2)^2 + m_A^2\Gamma_A^2} \frac{m_A \Gamma(A \to Zh)(m_A)}{\pi} \tag{18}$$

$$\frac{d\sigma(b\bar{b} \to Zh)}{d\sqrt{s}} = \sigma(b\bar{b} \to A)(s) \frac{2\sqrt{s}}{(s - m_A^2)^2 + m_A^2\Gamma_A^2} \frac{\sqrt{s}\Gamma(A \to Zh)(s)}{\pi}, \tag{19}$$

where $\Gamma(A \to Zh) = \Gamma_A \times \mathrm{BR}(A \to Zh)$. The only difference between those two formulas is that in Eq. (18) we are choosing $\sigma(b\bar{b} \to A)$ cross section and $\Gamma(A \to Zh)$ to be on shell. The s - dependence is only in the propagator-squared-like part. On the other hand in Eq. (19) both cross section and $A \to Zh$ decay width depend on the center of mass energy.

The results of applying approximation formulas Eqs. (18) and (19) at LO are shown in Figures 5 - 7. For masses $M_A = 250$ GeV and 400 GeV both formulas are in a good agreement, while for 1000 GeV there is a shift of approximately 100 GeV.

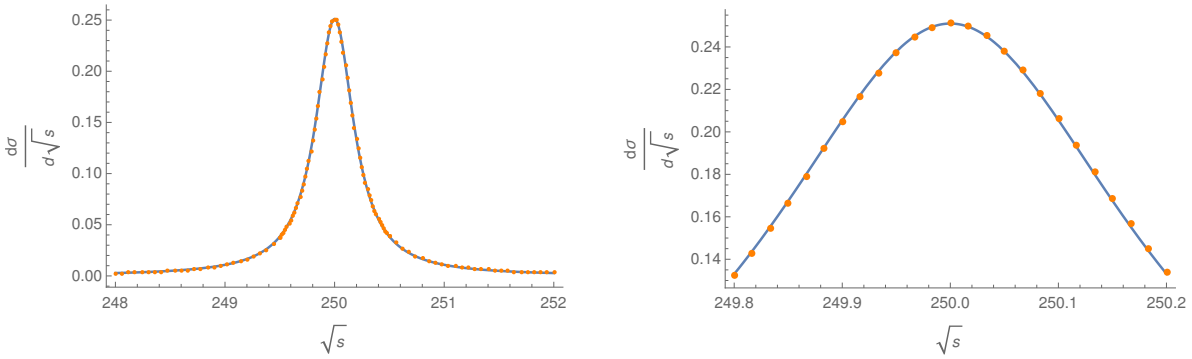

Figure 5: $M_A = 250$ GeV, $\tan\beta = 2$, $\sin(\alpha - \beta) = 0.6$
solid blue line corresponds to the formula (18), dotted line - to the formula (19)

To check how well those approximations work we also compared Eqs. (18) and (19) results with the analytical answer. According to our calculations both formulas are doing an equally good job for the pseudoscalar masses 250 GeV and 400 GeV (relatively small decay widths). On the other hand only formula (19) agrees with the analytical result for 1000 GeV. However such an observation is not surprising at all since when we are dealing with narrow peaks we can neglect the s–dependence of $\sigma(b\bar{b} \to A)$ and $\Gamma(A \to Zh)$. As a consequence both formulas give very close results. For huge widths one should take into account s–dependence and use the improved approximation in Eq. (19).

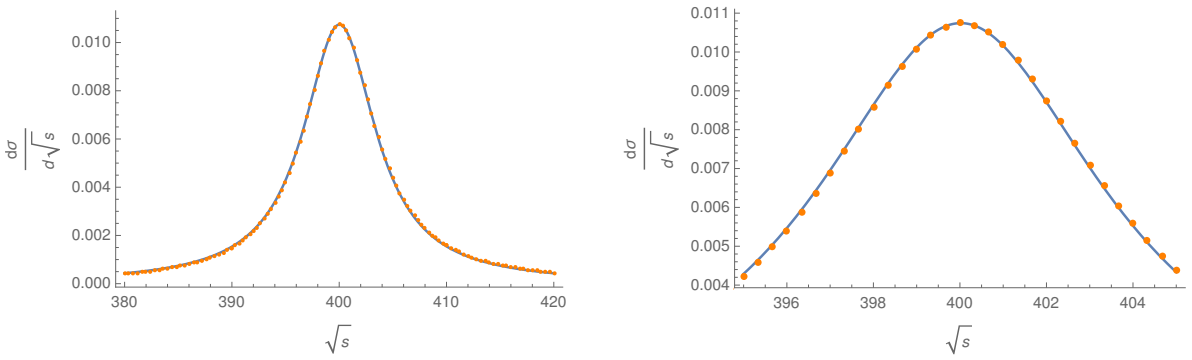

Figure 6: $M_A = 400$ GeV, $\tan\beta = 6$, $\sin(\alpha - \beta) = 0.8$
solid blue line corresponds to the formula (18), dotted line - to the formula (19)

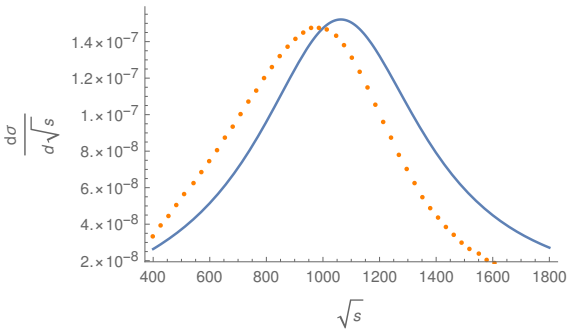

Figure 7: $M_A = 1000$ GeV, $\tan\beta = 5$, $\sin(\alpha - \beta) = 0.9$
solid blue line corresponds to the formula (18), dotted line - to the formula (19)

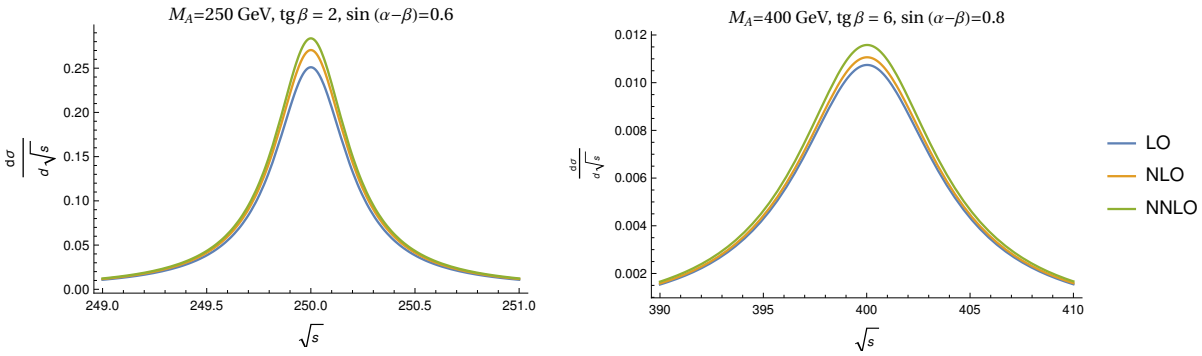

Figure 8: Comparison between the LO, NLO and NNLO calculations with formula (18) for two benchmark points

Since we have found that our approximation formulas are in a good agreement with analytical calculation, we used Eqs. (18), (19) and `SusHi` to obtain cross sections $\sigma(pp \to A)$ up to NNLO. Fig. 8 shows our results for $\frac{d\sigma}{d\sqrt{s}}$ (250 and 400 GeV). Here Eq. (18) was used. Fig. 9 shows the result for 1000 GeV based on the approximation formula Eq. (19).[1]

[1]At LO the improved formula is exactly identical to our analytical calculation. However, since formula (19) is taking into account only production and decay corrections, if there are diagrams connecting initial and final state those are all neglected. In our case of the $b\bar{b} \to A \to Zh$ process there are no such diagrams at NLO, since QCD corrections can only occur only in production. Beyond NLO some diagrams are neglected in our calculation.

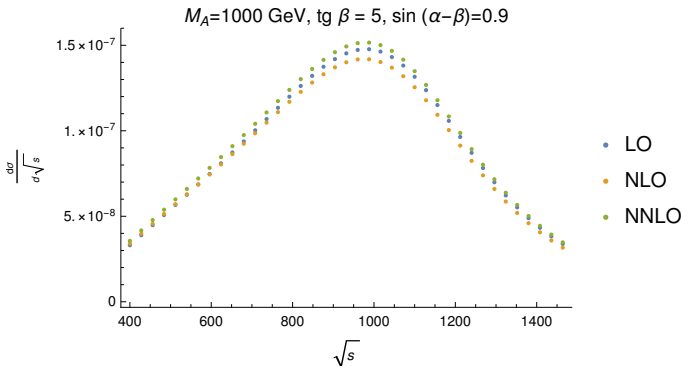

Figure 9: Comparison between the LO, NLO and NNLO calculations with formula (19) for the benchmark point with $M_A = 1000$ GeV

6 Conclusion

This work contains a study of the $b\bar{b} \to A \to Zh$ process in hadron collisions. We have given a brief overview of the THDM and illustrated the model dependence on the input parameters such as pseudoscalar mass M_A and mixing angles β and α in form of $\tan\beta$ and $\cos(\alpha - \beta)$. Also we have performed an analytical calculation of the cross section $\sigma\left(b\bar{b} \to A \to Zh\right)$ at LO, that we evaluated numerically for three points in parameter space shown in Table 2. We have proven that the approximation formulas given with Eq. (18) and Eq. (19) are working well. Those formulas are based on splitting the process to A–production (can be numerically calculated with `SusHi`) and the subsequent A–decay (can be calculated with `2HDMC`). Finally, we have applied the approximations Eqs. (18) and (19) to perform a calculation of the studied process up to NNLO.

Future steps of this work could contain the analytical calculation of the whole process $b\bar{b} \to Zh$. This process apart from $b\bar{b} \to A \to ZH$ also contains diagrams with internal Z–boson and internal b–quarks in the t– and u–channel.

7 Acknowledgments

I would like to acknowledge Stefan Liebler and Emanuele Bagnaschi for their intensive support, help and patience during all summer program, for our fruitful discussions and for answering my questions, Georg Weiglein for supervising me. Also I would like to thank the whole theory group for being hospitable and caring.

Additionally, I would like to express my gratitude to Olaf Behnke and the whole DESY Summer Student organization team for this amazing academic and social experience in Hamburg.

8 References

[1] Gustavo Castelo Branco, PM Ferreira, L Lavoura, MN Rebelo, Marc Sher, and Joao P Silva. Theory and phenomenology of two-higgs-doublet models. *Physics reports*, 516(1):1–102, 2012.

[2] Andy Buckley, James Ferrando, Stephen Lloyd, Karl Nordström, Ben Page, Martin Rüfenacht, Marek Schönherr, and Graeme Watt. Lhapdf6: parton density access in the lhc precision era. *The European Physical Journal C*, 75(3):132, 2015.

[3] D Benjamin Clark, Eric Godat, and Fredrick I Olness. Maneparse: a mathematica reader for parton distribution functions. *Computer Physics Communications*, 216:126–137, 2017.

[4] David Eriksson, Johan Rathsman, and Oscar Stål. 2hdmc–two-higgs-doublet model calculator. *Computer physics communications*, 181(1):189–205, 2010.

[5] Robert V Harlander, Stefan Liebler, and Hendrik Mantler. Sushi: A program for the calculation of higgs production in gluon fusion and bottom-quark annihilation in the standard model and the mssm. *Computer Physics Communications*, 184(6):1605–1617, 2013.

[6] Robert V Harlander, Stefan Liebler, and Hendrik Mantler. Sushi bento: Beyond nnlo and the heavy-top limit. *Computer Physics Communications*, 212:239–257, 2017.

[7] Robert V Harlander, Stefan Liebler, and Tom Zirke. Higgs strahlung at the large hadron collider in the 2-higgs-doublet model. *Journal of High Energy Physics*, 2014(2):23, 2014.

[8] Michael Edward Peskin. *An introduction to quantum field theory*. Westview press, 1995.

[9] Georg Weiglein and Stefan Liebler. Lecture notes on higgs physics. 2016.